Chemical Engineering Journal 155 (2009) 647–653

Contents lists available at ScienceDirect

Chemical Engineering Journal

journal homepage: www.elsevier.com/locate/cej

Removal of lead copper chromium and cobalt ions onto granular activated carbon in batch and fixed-bed adsorbers

Abbas H. Sulaymon [a], Balasim A. Abid [b], Jenan A. Al-Najar [b,*]

[a] Environment Engineering Department, College of Engineering, University of Baghdad, Al Sunaha Street, Baghdad, Iraq
[b] Chemical Engineering Department, University of Technology, Baghdad, Iraq

ARTICLE INFO

Article history:
Received 8 April 2009
Received in revised form 4 August 2009
Accepted 24 August 2009

Keywords:
Adsorption
Activated carbon
Lead
Copper
Chromium
Cobalt

ABSTRACT

The adsorption of lead, copper, chromium and cobalt ions onto granular activated carbon (DARCO 20–40 mesh) in a single component system has been studied using fixed-bed adsorbers. A film-pore diffusion model has been utilized to predict the fixed-bed breakthrough curves for each of the four metal ions. This model considers both external and internal mass transfer resistances as well as axial dispersion with non-linear isotherm. The effects of flow rate, bed height and initial metal ion concentration on the breakthrough curves have been studied. The equilibrium isotherm data, the external mass transfer coefficient and pore diffusion coefficient were obtained from separate experiments in batch adsorber by fitting the experimental data with theoretical model. The pore diffusion coefficient was obtained using pore diffusion model for batch adsorber by matching between the experimental data and the model predicted data. The results show that the film-pore diffusion model used for fixed-bed adsorber provides a good description of adsorption process for Pb(II), Cu(II), Cr(III) and Co(II) onto activated carbon in fixed-bed adsorber.

1. Introduction

Heavy metals are among the most toxic contaminants of surface water. The main sources of toxic metals are industrial wastes from processes such as electroplating, metal finishing and chemical manufacturing.

Since all heavy metals are non-degradable into nontoxic metal end products, these concentrations must be reduced to acceptable levels before being discharged into the environment. Otherwise these could pose threat to public health and/or affect the quality of potable water [1]. Effect of metals and their compounds on humans, animals and plants, is quite varied. Human metal intake may occur primarily from contaminated food, drinking water, skin and lung adsorption. According to WHO [2] and IPCS [3], the most toxic metals are aluminum, chromium, cobalt, nickel, copper, zinc, cadmium, mercury and lead.

A number of treatment methods for removing heavy metals from industrial wastewater include chemical precipitation, ion exchange, filtration, membrane separation and adsorption. Among them adsorption is found to be the most effective method for removing dissolved metal ions from wastes [1].

Adsorption is the most commonly used process because it is fairly simple and convenient unit operation and that the cost for its application is relatively low compared to other treatment processes. Use of adsorption contacting system for industrial and municipal wastewater treatment has become prevalent during recent years [4]. Adsorption is often used at the end of a treatment sequence for pollution control due to the high degree of purification that can be achieved. Activated carbon is the most popular adsorbent used for the application of adsorption technique [5].

Fixed-bed adsorber is the most efficient arrangement for conducting adsorption operation for industrial applications in the wastewater treatment [5]. The kinetics behavior of fixed-bed adsorber can be explained and the characteristic breakthrough curve of the adsorption phenomenon can be obtained through mathematical models. A number of mathematical models have been developed to explain the kinetic behavior of the fixed-bed adsorber and to estimate the breakthrough curve [5,6]. The mechanism of adsorption onto an adsorbent includes external diffusion, internal diffusion and adsorption onto the porous surface. Several models have been developed take into account an external film diffusion step, internal diffusion and non-linear equilibrium isotherm to predict adsorption rate in a batch adsorber and fixed-bed adsorber [7].

Both batch adsorption and fixed-bed adsorption studies are required to obtain key parameters required for the design of

* Corresponding author at: Chemical Engineering Department, University of Technology, P.B. 3510, Baghdad, Iraq. Tel.: +964 780 905 7510.
E-mail address: jenan_iraqi@yahoo.com (J.A. Al-Najar).

1385-8947/$ – see front matter © 2009 Elsevier B.V. All rights reserved.
doi:10.1016/j.cej.2009.08.021

Nomenclature

b	adsorption equilibrium constant (m^3/kg)
Bi	Biot no. ($k_f R_p/\varepsilon_p D_p$)
C	fluid phase concentration (kg/m^3)
C_e	equilibrium liquid-phase concentration, (kg/m^3)
C_o	initial liquid-phase concentration (kg/m^3)
D_L	axial dispersion coefficient (m^2/s)
D_m	molecular diffusivity (m^2/s)
D_p	pore diffusion coefficient (m^2/s)
d_p	particle diameter (m)
k_f	external mass transfer coefficient (m/s)
L	length of the column (m)
n	constant in Freundlich equation
Pe	Peclet number, ($\nu L/D_L$)
q_e	adsorption capacity at equilibrium (kg/kg)
q_m	Langmuir constant (kg/kg)
r	radial coordinate (m)
R	radial coordinate (m)
R_e	Reynolds number, $Re = \rho_w \nu d_p/\mu_w$
R_p	radius of particle (m)
Sc	Schmidt number ($Sc = \mu_w/\rho_w D_m$)
Sh	Sherwood number ($sh = k_f d_p/D_m$)
t	time (s)
V	volume of the solution (m^3)
W	mass of granular activated carbon (kg)
Z	axial distance (m)
ε_b	bed porosity
ε_p	porosity of adsorbent
ζ	dimensionless group in Eq. (15) $\zeta = 3Bi\eta(1-\varepsilon_b)/\varepsilon_b$
η	dimensionless group in Eq. (15) $\zeta = \varepsilon_p D_p L/R_p^2 \nu$
μ_w	viscosity of water (Pa s)
ν	interstitial velocity ($Q/\pi R_p^2 \varepsilon_b$) (m/s)
ρ_w	density of water (kg/m^3)
ρ_p	particle density (kg/m^3)

Subscript

b	bulk-fluid phase
e	equilibrium
GAC	granular activated carbon
L	liquid phase
o	initial
p	particle phase

fixed-bed adsorber. Batch adsorption studies were performed to obtain the key parameters such as isotherm constants and the pore diffusivity. Fixed-bed adsorption is used to determine experimental breakthrough curve.

In the present study, film-pore diffusion model is used to determine the breakthrough curves in fixed-bed column for single component adsorption onto granular activated carbon and compare the experimental results with that simulated by numerical simulation of the film-pore diffusion model, which includes film mass transfer, pore diffusion resistance, axial dispersion and non-linear isotherms.

2. Mathematical model

A number of mathematical models have been developed to describe the dynamic behavior of fixed-bed adsorber and to estimate the breakthrough curve. Outside the adsorbent particle, metal ions are transported via axial dispersion and film diffusion from the bulk-fluid to the particle surface. Inside the particle, metal ions diffuse into the inner portion of the particle via surface diffusion, pore diffusion or both.

In the present study, film-pore diffusion model is utilized to predict the fixed-bed breakthrough curves for single metal ion adsorbed onto porous media. The model takes account of: external mass transfer resistance, internal mass transfer resistance, non-ideal plug flow and non-linear isotherm [6,8].

The following basic assumptions are made to formulate the pore diffusion model [6]:

- The system operates under isothermal conditions.
- The equilibrium of the adsorption is described by Langmuir isotherm.
- Solid particles are spherical, uniform in size and density. They also do not swell or shrink.
- No radial concentration gradient in the column and no angular concentration gradient within a particle.
- The intraparticle mass transfer is due to Fickian diffusion and it is characterized by the constant pore diffusion coefficient, D_p.
- Mass transfer across the boundary layer surrounding the solid particles is characterized by the external film mass transfer coefficient k_f.
- All the mechanisms that contribute to axial mixing are lumped together into a single axial dispersion coefficient.

Continuity equation in the bulk-fluid:

$$-D_L \frac{\partial^2 C_b}{\partial Z^2} + \nu \frac{\partial C_b}{\partial Z} + \frac{\partial C_b}{\partial t} + \rho_p \left(\frac{1-\varepsilon_b}{\varepsilon_b}\right) \frac{\partial q}{\partial t} = 0 \quad (1)$$

The following initial and boundary conditions are considered:

$$\text{I.C.}: \quad C_b = C_{bo}, \quad Z = 0, \quad t = 0 \quad (2)$$

$$C_b = 0, \quad 0 < Z \le L, \quad t = 0 \quad (3)$$

$$\text{B.C.}: \quad D_L \frac{\partial C_b}{\partial Z} = -\nu(C_{bo} - C_b), \quad Z = 0, \quad t > 0 \quad (4)$$

$$\frac{\partial C_b}{\partial Z} = 0, \quad Z = L, \quad t \ge 0 \quad (5)$$

Using C_b the concentration in the stagnant fluid inside the macropore, the inter-phase mass transfer rate may be expressed as

$$\rho_p \frac{\partial q}{\partial t} = \frac{3k_f}{R_p}(C_b - C_{p,R=R_p}) \quad (6)$$

Substituting of Eq. (6) into Eq. (1) gives

$$-D_L \frac{\partial^2 C_b}{\partial Z^2} + \nu \frac{\partial C_b}{\partial Z} + \frac{\partial C_b}{\partial t} + \frac{3k_f(1-\varepsilon_b)}{\varepsilon_b R_p}(C_b - C_{p,R=R_p}) = 0 \quad (7)$$

The particle continuity equation in spherical coordinates is as follows:

$$\varepsilon_p \frac{\partial C_p}{\partial t} + (1-\varepsilon_p)\rho_p \frac{\partial q}{\partial t} - \varepsilon_p D_p \left(\frac{\partial^2 C_p}{\partial R^2} + \frac{2}{R}\frac{\partial C_p}{\partial R}\right) = 0 \quad (8)$$

The following initial and boundary conditions are considered:

$$\text{I.C.}: \quad C_p = 0, \quad q = 0, \quad R = 0, \quad t = 0 \quad (9)$$

$$\text{B.C.}: \quad \frac{\partial C_p}{\partial R} = 0, \quad R = 0, \quad t > 0 \quad (10)$$

$$D_p \frac{\partial C_p}{\partial R} = k_f(C_b - C_{P,R=Rp}), \quad R = R_p, \quad t \ge 0 \quad (11)$$

Since equilibrium is assumed for adsorption at the interior site, q and C_p in Eq. (8) are related by the instantaneous equilibrium expression

$$\frac{\partial q}{\partial t} = \frac{\partial q}{\partial C_p}\frac{\partial C_p}{\partial t} \quad (12)$$

Using Eq. (12) with Eq. (8) and rearranging Eq. (8) yield:

$$\frac{\partial C_p}{\partial t} = \frac{1}{1+\rho_p[(1-\varepsilon_p)/\varepsilon_p](\partial q/\partial C_p)} D_p \left(\frac{\partial^2 C_p}{\partial R^2} + \frac{2}{R}\frac{\partial C_p}{\partial R} \right) \quad (13)$$

The adsorption isotherm is non-linear and described by Langmuir isotherm model:

$$q = \frac{q_m b C_p}{1+bC_p} \quad (14)$$

Defining the following dimensionless variables:

$$c_b = \frac{C_b}{C_o}, \quad c_p = \frac{C_p}{C_o}, \quad q^\bullet = \frac{\rho_p q}{C_o}, \quad \tau = \frac{\nu t}{L}, \quad r = \frac{R}{R_p}, \quad z = \frac{Z}{L}$$

The dimensionless parameters are defined as

$$Pe = \frac{\nu L}{D_L}, \quad Bi = \frac{k_f R_p}{\varepsilon_p D_p}, \quad \eta = \frac{\varepsilon_p D_p L}{R_p^2 \nu}, \quad \zeta = \frac{3Bi\eta(1-\varepsilon_b)}{\varepsilon_b}$$

Eqs. (7) and (2)–(5), can be transformed into the following dimensionless equations:

$$-\frac{1}{Pe}\frac{\partial^2 c_b}{\partial z^2} + \frac{\partial c_b}{\partial z} + \frac{\partial c_b}{\partial \tau} + \zeta(c_b - c_{p,r=1}) = 0 \quad (15)$$

I.C.:

$$c_b = 1, \quad z = 0, \quad \tau = 0 \quad (16)$$

$$c_b = 0, \quad 0 < z \leq 1, \quad \tau = 0 \quad (17)$$

B.C.:

$$\frac{\partial c_b}{\partial z} = -Pe(1-c_b), \quad z = 0, \quad \tau > 0 \quad (18)$$

$$\frac{\partial c_b}{\partial z} = 0, \quad z = 1, \quad \tau \geq 0 \quad (19)$$

Eqs. (13), (14) and (9)–(11) can be transformed into the following dimensionless equations:

$$\frac{\partial c_p}{\partial \tau} = \frac{1}{\varepsilon_p + (1-\varepsilon_p)(\partial q^\bullet/\partial c_p)} \eta \left(\frac{\partial^2 c_p}{\partial r^2} + \frac{2}{r}\frac{\partial c_p}{\partial r} \right) \quad (20)$$

$$q^\bullet = \frac{\rho_p q_m b c_p}{1+bc_p C_o} \quad (21)$$

$$\text{I.C.}: \quad c_p = 0, \quad q^\bullet = 0, \quad r = 0, \quad \tau = 0 \quad (22)$$

$$\text{B.C.}: \quad \frac{\partial c_p}{\partial r} = 0, \quad r = 0, \quad \tau > 0 \quad (23)$$

$$\frac{\partial c_p}{\partial r} = Bi(c_b - c_{P,r=1}), \quad r = 1, \quad \tau \geq 0 \quad (24)$$

Since non-linear adsorption equilibrium (Langmuir isotherm) is considered, the preceding set of partial differential equations (Eqs. (15)–(24)) are solved numerically by reduction to a set of ordinary differential equations using finite element method for bulk-fluid partial differential equation and the orthogonal collocation method for the particle phase equations. The ordinary differential equation system with initial values can be readily solved using an ordinary differential equation solver such as the subroutine "ODE15S" OF MATLAM v. 7 which is a variable order solver based on the numerical differentiation formulas (NDFs).

3. Experimental materials and procedure

3.1. Adsorbate

1000 mg/l standard stock solution of each metal ions of Pb(II), Cu(II), Cr(III) and Co(II) were prepared by dissolving $Pb(NO_3)_2$, $Cu(NO_3)_2{\cdot}3H_2O$, $Co(NO_3)_2{\cdot}6H_2O$, $Cr(NO_3)_3{\cdot}9H_2O$ respectively in distilled water. The chemicals used are annular grade produced by Fluka and Aldrich–Sigma

Table 1
Physical properties of granular activated carbon.

Product name	Activated carbon, DARACO 20-40 mesh, granular
Company	Sigma–Aldrich Company (UK) Ltd.
Composition	Carbon C
Bulk density, kg/m^3	336
BET surface area, m^2/g	603
Average pore diameter, nm	3.72
pH	6.9

3.2. Adsorbent

The granular activated carbon (supplied by Sigma–Aldrich Com., United Kingdom) was used. Granular activated carbon (GAC) was used directly without any treatment. The mean diameter of the GAC particles is 0.6 mm. The physical properties were measured at Thermochemistry Laboratory, Chemical Science (Faculty of Health and Medical Science), University of Surrey, United Kingdom and are presented in Table 1.

3.3. Procedure

The initial pH of the experiments were adjusted at 5.5, 5.5, 3 and 6 for Pb(II), Cu(II), Cr(III) and Co(II) respectively. These were carried out by using 0.1 M NaOH and 0.1 M HCl.

The fixed-bed experiments were carried out in Perspex glass column of 38.1 mm (I.D.) and 40 cm in height with perforated plate at the bottom of the column to support the activated carbon bed and a solution distributor at the top of the column. Plastic beads with depth 3 cm were placed at the top of the activated carbon bed to ensure a uniform distribution of the influent through the activated carbon bed. Feed tank of 2 l was used, which is placed at the top of the adsorber. Feed solution with desired concentration were prepared in feed tank and introduced to the column through the solution distributor. More details on the fixed-bed experiments are given in [9].

For the determination of adsorption isotherm, a volume of 10 ml of metal ion solution with different initial concentration of 10–200 mg/l was placed in ten test tubes containing a known mass of activated carbon. The test tubes were then shaken at a constant speed of 250 r.p.m. in a water bath at 25 °C ± 1 for 24 h. After shaking, the activated carbon was separated by means of centrifuge and then filtrate through a membrane filter (0.45 μm). The filtrate was analyzed for the remaining metal ion concentration by atomic absorption spectrometer AAS. The adsorbed amount is (q_e) calculated by the following equations:

$$q_e = \frac{V}{W}(C_o - C_e) \quad (25)$$

$$q_e = f(C_e) \quad (26)$$

The pore diffusion coefficient for each solute was obtained by 1 l Pyrex beaker fitted with a variable speed mixer. The beaker was filled with 0.5 l of known concentration solution and the agitation started before adding GAC. At time zero, the calculated weight of activated carbon was added and then samples were taken at every 5 min.

The weight of activated carbon used to reach equilibrium related concentration of C_o/C_e equal 0.05 is calculated from isotherms model and mass balance equation (Eqs. (25) and (26)).

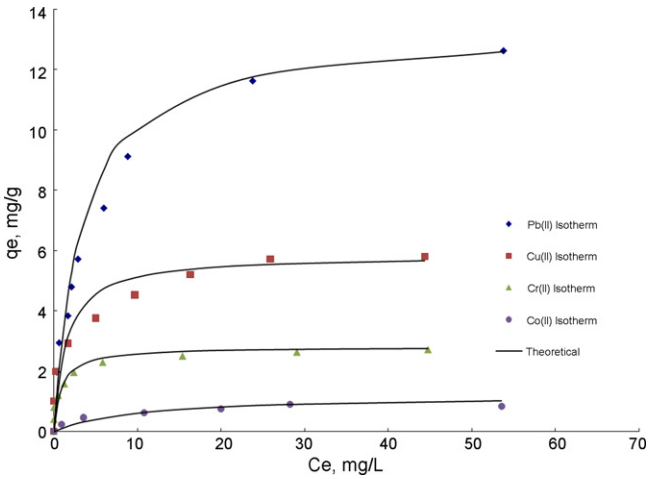

Fig. 1. Adsorption isotherm for Pb(II), Cu(II), Cr(III) and Co(II) onto activated carbon, Temp. = 25 °C.

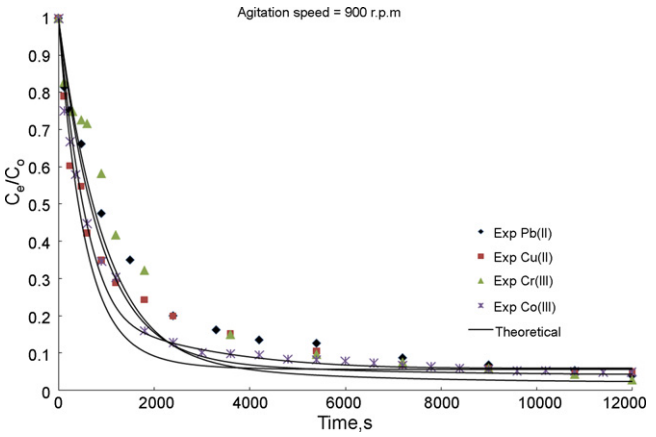

Fig. 2. Comparison of the measured concentration-time decay data with that predicted by pore diffusion model for Pb(II), Cu(II), Cr(III) and Co(II) in batch adsorber.

4. Results and discussion

4.1. Adsorption isotherm

The adsorption isotherm curves were obtained by plotting the weight of the solute adsorbed per unit weight of the adsorbent (q_e) against the equilibrium concentration of the solute (C_e). Fig. 1 shows the adsorption isotherm curves for single metal ions Pb(II), Cu(II), Cr(III) and Co(II) onto activated carbon at 25 °C respectively.

The adsorption for each metal ions show non-linear dependence on the equilibrium concentration. The equilibrium isotherm curves of Pb(II) and Cu(II), Cr(III) and Co(II) is of favorable type. The experimental adsorption data for all the metal ions used were correlated with four isotherm model, Langmuir model ($R^2 = 0.99$), Freundlich model ($R^2 = 0.97$), Redlich–Peterson model ($R^2 = 0.98$) and combination of Langmuir–Freundlich model ($R^2 = 0.99$). The correlation coefficient (R^2) between the experimental data and the theoretical models was very good for all system. The Langmuir isotherm model was used in the fixed-bed model. The Langmuir parameters q_m and, b are evaluated to be as follows:

- Pb(II): $q_m = 13.333$ mg/g, $b = 0.312$ l/mg;
- Cu(II): $q_m = 5.845$ mg/g, $b = 0.710$ l/mg;
- Cr(III): $q_m = 2.793$ mg/g, $b = 1.144$ l/mg;
- Co(II): $q_m = 1.193$ mg/g, $b = 0.105$ l/mg.

4.2. Pore diffusion coefficient

Pore diffusion coefficient D_p of each metal ions can be obtained using batch model by matching the concentration decay curve obtained from experimental data at optimum agitation (900 r.p.m.) speed with that obtained from the batch model as shown in Fig. 2. Batch model used either pore diffusion model or surface diffusion model. At the first time the pore diffusion model is assumed and the model is solved numerically. If there is no matching between the experimental and theoretical result then the surface diffusion model must be used instead. This matching was made by minimizing the differences between the theoretical and the experimental concentration decay curve. In the present work pore diffusion model give matching with the experimental data. The principal parameter required for solving the batch model is the external mass transfer coefficient k_f and pore diffusion coefficient D_p. the following steps must be made to introduce the required parameter and conditions:

- Estimate the optimum concentration decay curve at optimum agitation speed.
- Numerical solution of the batch model can be used to obtain the theoretical concentration decay curve.
- Matching between the experimental and the theoretical concentration decay curve.

The pore diffusion coefficient for each metal ions are evaluated from batch experiments to be

- Pb(II): $D_p = 7.955 \times 10^{-10}$ m^2/s.
- Cu(II): $D_p = 3.532 \times 10^{-10}$ m^2/s.
- Cr(III): $D_p = 2.266 \times 10^{-10}$ m^2/s.
- Co(II): $D_p = 1.316 \times 10^{-10}$ m^2/s.

The amount of GAC used for each metal ions were calculated for final equilibrium related concentration of $C_e/C_o = 0.05$, using the Langmuir isotherm with mass balance in 1 l of solution. The initial concentration were 60, 100, 100 and 60 mg/l with the doses of activated carbon of 10, 20, 50 and 180 g per 1 l of solution for Pb(II), Cu(II), Cr(III) and Co(II) respectively. The external mass transfer coefficient, k_f, in packed bed column model was calculated (4.202×10^{-6}, 2.982×10^{-6}, 0.718×10^{-6} and 0.347×10^{-6} m/s for Pb(II), Cu(II), Cr(III) and Co(II) respectively) using the correlation of Wilson and Geankoplis [10]. The molecular diffusion coefficient D_m is 1.43×10^{-9} m^2/s [11].

$$Sh = \frac{1.09}{\varepsilon_b} Re^{1/3} Sc^{1/3} \quad \text{for } 0.0015 < Re < 55 \tag{27}$$

The axial dispersion coefficient, D_L, calculated at different flow rate (4.172×10^{-6}, 6.193×10^{-6} and 8.186×10^{-6} m^2/s at 0.667, 1 and 1.33 ml/s respectively) from Chung and Wen equation [12]:

$$\frac{vL}{D_L} = \frac{L}{2R_p\varepsilon_b}(0.2 + 0.011Re^{0.48}) \tag{28}$$

4.3. Effect of flow rate

Figs. 3–5 show the experimental and predicted breakthrough curves for Pb(II), Cu(II) and Co(II) respectively obtained for different flow rates (0.667, 1 and 1.333 ml/min) in terms C_e/C_o versus time.

It is clear from these figures that as the flow rate increases the time of breakthrough point decreases. This is because the residence time of solute in the bed decreases as the flow rate increases, therefore there is not enough time for adsorption equilibrium to be reached which results in lower bed utilization and the adsorbate solution leaves the column before equilibrium. It is expected

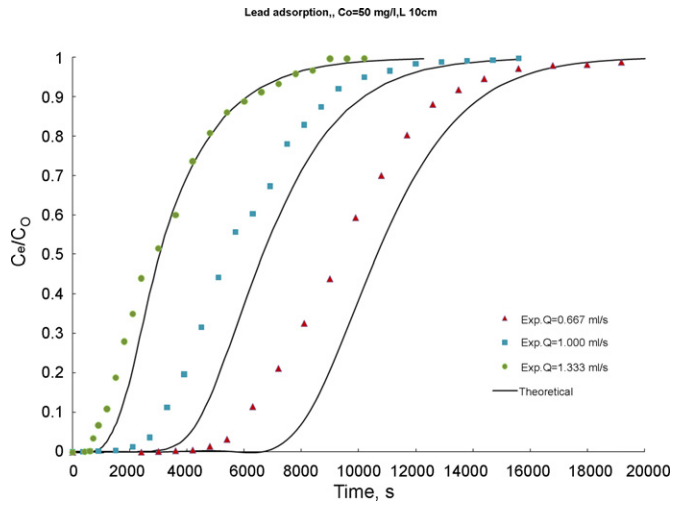

Fig. 3. The experimental and predicted breakthrough curves for adsorption of Pb(II) onto activated carbon at different flow rates.

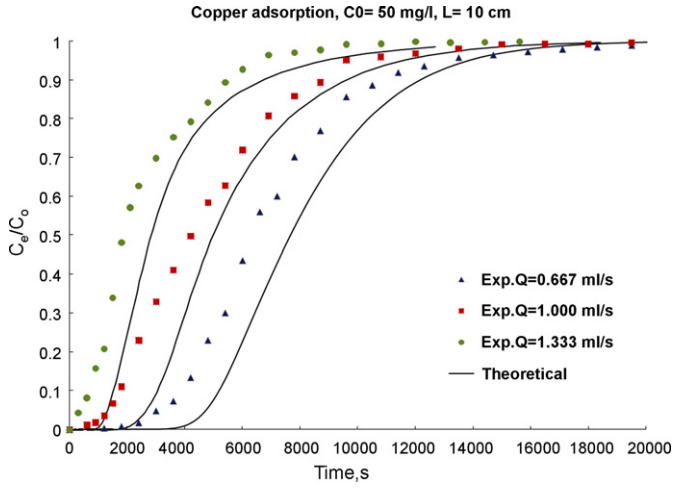

Fig. 4. The experimental and predicted breakthrough curves for adsorption of Cu(II) onto activated carbon at different flow rates.

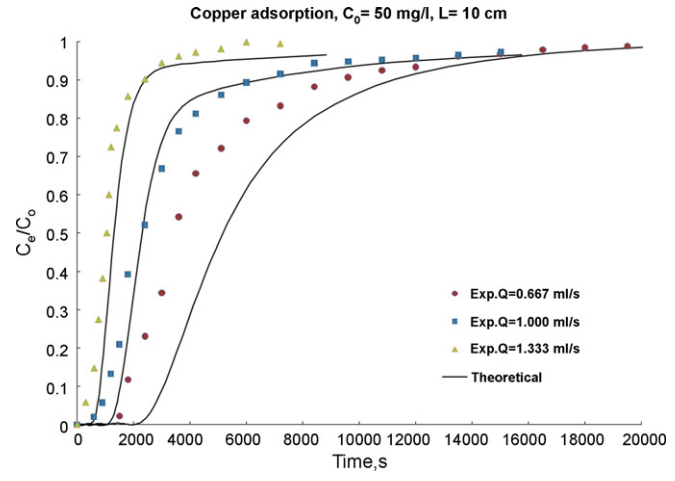

Fig. 5. The experimental and predicted breakthrough curves for adsorption of Co(II) onto activated carbon at different flow rates.

Table 2
The values of Biot no. and Peclet no. at different flow rates.

Metal ions	Flow rate (Q, ml/s)	Biot no. (Bi)	Peclet no. (Pe)
Pb(II)	0.667	41.54	35.06
	1.000	47.54	35.43
	1.330	52.32	35.74
Cu(II)	0.667	93.56	35.06
	1.000	107.08	35.43
	1.330	117.84	35.74
Co(II)	0.667	251.09	35.06
	1.000	287.39	35.43
	1.330	316.28	35.74

that the change in flow rate will affect the film diffusion but not the intraparticle diffusion. The higher the flow rate the smaller the film resistance to mass transfer and hence larger k_f results. Increasing flow rate at constant bed height will increase the Biot number with slight increases in Peclet number as listed in Table 2. Biot number is defined as the ratio of the external mass transfer to intraparticle mass transfer. When the Biot number is high the time of breakthrough point will appear early. The higher Biot number value indicates that the film diffusion is not dominating compared to the intraparticle mass transfer and the intraparticle mass transfer is the controlling step. These results are in agreement with that obtained by [6,11,13–15,17].

4.4. Effect of bed height

The bed height is one of the major parameters in the design of fixed-bed adsorption column. The effect of bed height on the breakthrough curve was studied for adsorption of Pb(II), Cu(II), Cr(III) and Co(II) respectively onto activated carbon. The experimental and predicted breakthrough curves obtained for different bed height of activated carbon (5, 10, 15 and 20 cm) at constant flow rate and constant initial concentration of metal ion are presented in Figs. 6–9. It is clear from these figures that at smaller bed height the C_e/C_o increases more rapidly than at a higher bed height. Furthermore at smaller bed height the bed is saturated in less time compared with the higher bed height. Smaller bed height means lesser amount of activated carbon than for the higher one.

Peclet number, Pe, is defined as the ratio of the axial convection rate to the axial dispersion rate. Increasing the bed height at constant flow rate increases Peclet numbers as listed in Table 3.

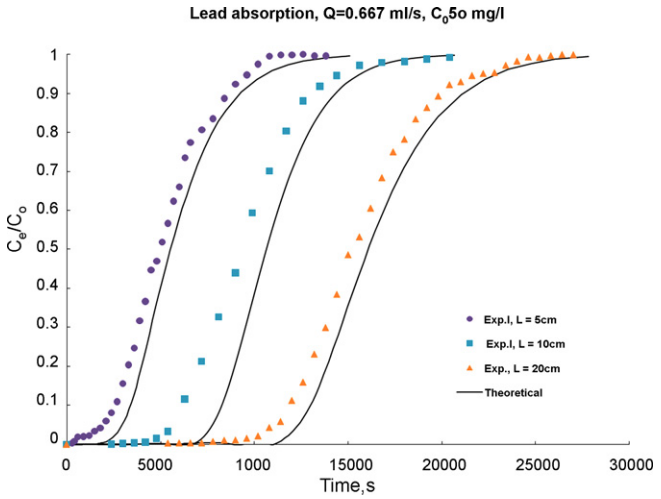

Fig. 6. The experimental and predicted breakthrough curves for adsorption of Pb(II) onto activated carbon at different bed heights.

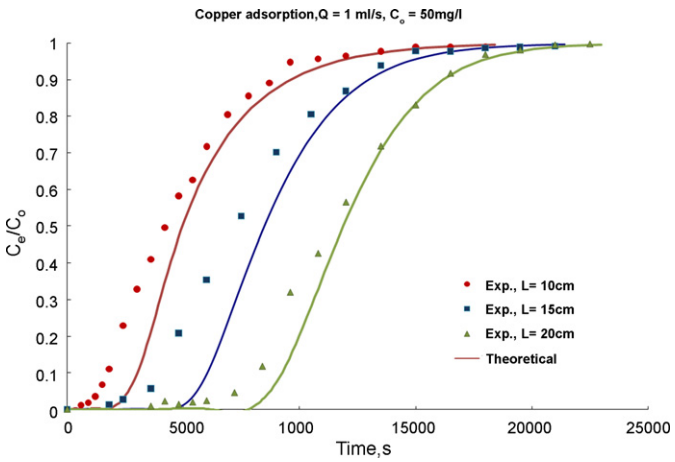

Fig. 7. The experimental and predicted breakthrough curves for adsorption of Cu(II) onto activated carbon at different bed heights.

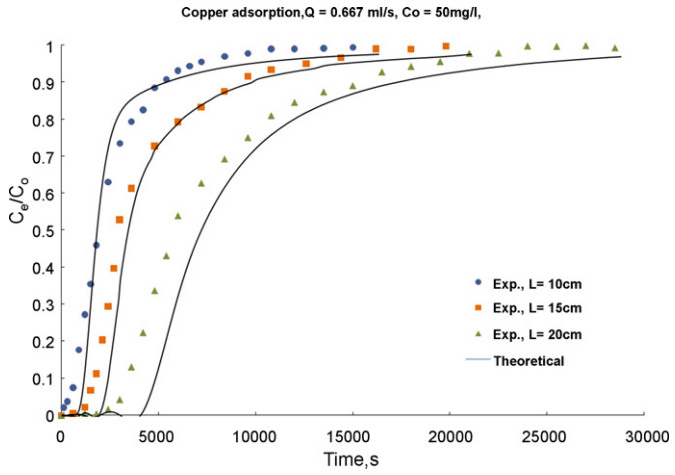

Fig. 8. The experimental and predicted breakthrough curves for adsorption of Cr(III) onto activated carbon at different bed heights.

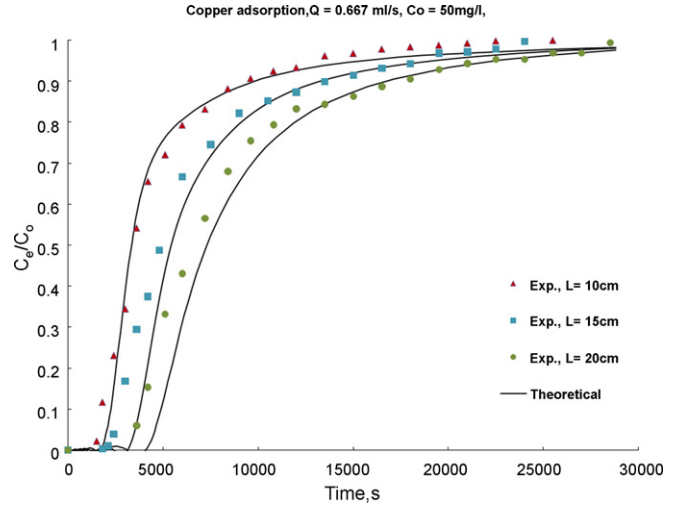

Fig. 9. The experimental and predicted breakthrough curves for adsorption of Co(II) onto activated carbon at different bed heights.

Table 3
The values of Biot no. and Peclet no. at different bed heights.

Metal ions	Bed height (cm)	Biot no. (*Bi*)	Peclet no. (*Pe*)
Pb(II)	5	41.54	17.53
	10	41.54	35.06
	20	41.54	70.11
Cu(II)	10	107.08	35.43
	15	107.08	53.14
	20	107.08	70.85
Cr(III)	10	83.5648	35.06
	15	83.5648	52.58
	20	83.5648	70.11
Co(II)	10	251.09	35.06
	15	251.09	52.58
	20	251.09	70.11

When the Peclet number is small the effect of axial dispersion is not negligible, the break point appears early and increases with the Peclet number. Hence, the internal and external resistances are confirmed to be the main parameters that control the adsorption kinetics with the increases in bed height. It is clear that increasing the bed height increases the breakthrough

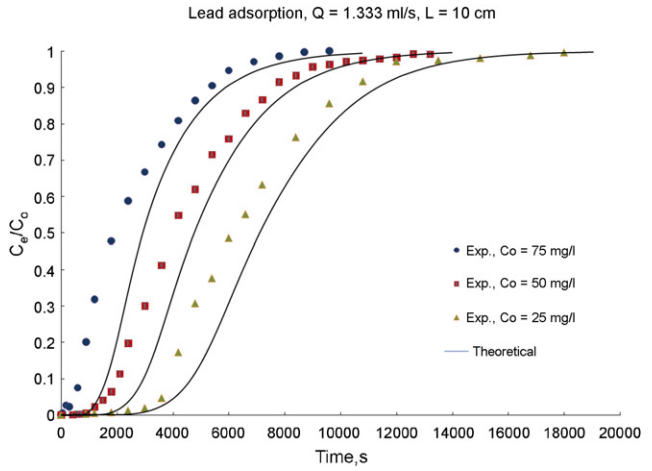

Fig. 10. The experimental and predicted breakthrough curves for adsorption of Pb(II) onto activated carbon at different initial metal ion concentrations.

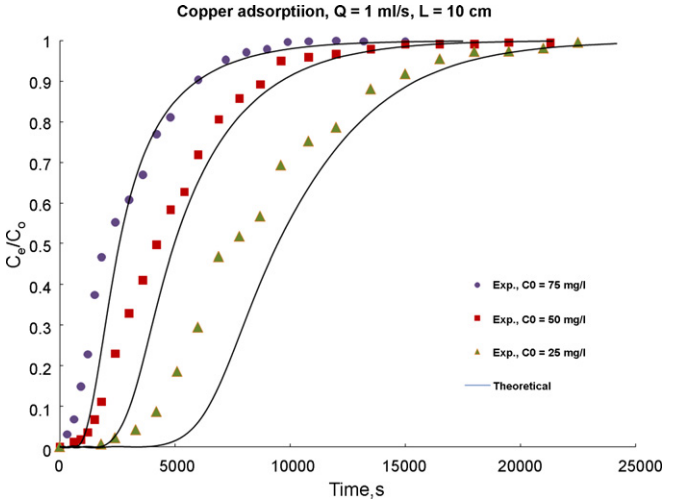

Fig. 11. The experimental and predicted breakthrough curves for adsorption of Cu(II) onto activated carbon at different initial metal ion concentrations.

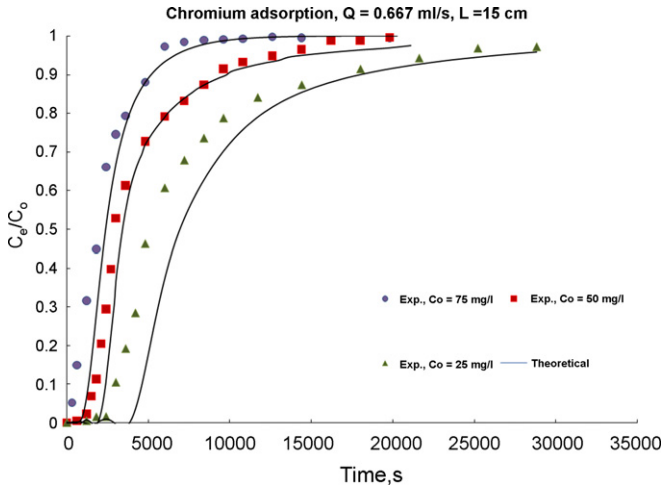

Fig. 12. The experimental and predicted breakthrough curves for adsorption of Cr(III) onto activated carbon at different initial metal ion concentrations.

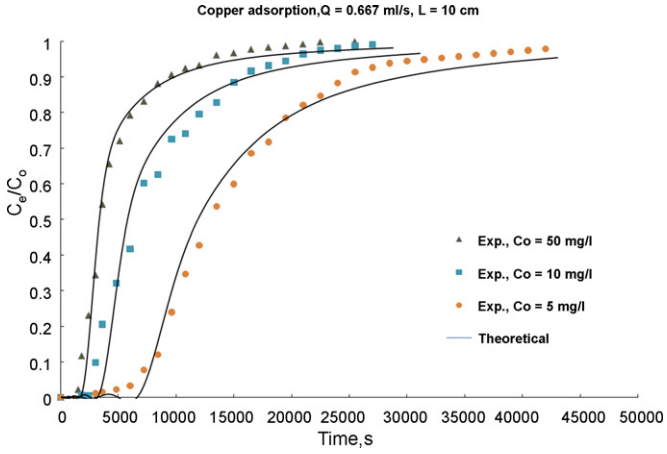

Fig. 13. The experimental and predicted breakthrough curves for adsorption of Co(II) onto activated carbon at different initial metal ion concentrations.

time and the residence time of the metal ion solution in the bed. These results are in agreement with the results obtained in Refs. [6,13–15].

4.5. Effect of initial concentration

The effect of initial metal ion concentration on the breakthrough curves for each metal ions Pb(II), Cu(II), Cr(III) and Co(II) was investigated for all systems. The change in initial metal ion concentration will have a significant effect on the breakthrough curves. Figs. 10–13 show the experimental and predicted breakthrough curves at different initial metal ion concentrations. These figures show that as the initial metal ion concentration increases the time of breakthrough point decreases. The higher the initial ion concentration, the faster the breakthrough; however, the activated carbon loadings are higher at higher initial metal ion concentration. For high initial metal ion concentration, steeper breakthrough curves are found because the equilibrium is attained faster, which would be anticipated with the basic that increases in the driving force for mass transfer with increases in initial metal ion concentration. Similar findings have been obtained in Refs. [11,13–17].

5. Conclusions

1. The granular activated carbon was found to be suitable adsorbent for the removal of Pb(II), Cu(II), Cr(III) and Co(II) from aqueous solution. The equilibrium isotherm curves of Pb(II), Cu(II), Cr(III) and Co(II) is of favorable type. The experimental data showed good fit to the Langmuir isotherm model. This adsorbent could be used effectively for the removal of these metal ions.
2. Pore diffusion model for batch adsorber is used to estimate the pore diffusion coefficient by matching the experimental concentration decay curve with the theoretical concentration decay curve obtained from the model.
3. Film-pore diffusion model has been successfully used to describe the adsorption process and to predict the breakthrough curve in fixed-bed column with granular activated carbon.
4. Fixed bed studied indicates that as the flow rate and the initial metal ion concentration increase, and the bed height decreases, the time of the breakthrough point decreases. These results improve the understanding of adsorption phenomena with reference to pore diffusion and are very useful in the design of adsorption column.

Acknowledgements

We thank Prof. Adel O. Sharif and Prof. Angela F. Danil de Namor, from University of Surrey in UK, for providing the space and all facilities needed in our work in the University of Surrey.

References

[1] M.M. Aslam, I. Hassan, M. Malik, A. Matin, Removal of copper from industrial effluent by adsorption with economical viable material, Electron. J. Environ. Agric. Food Chem. 3 (2004) 658–664, ISSN: 1579-4377.
[2] WHO, World Health Organization, Geneva Guidelines for Drinking Water Quality, 1984.
[3] IPCS, International Programme on Chemical Safety Environmental Health Criteria World Health Organization Geneva, 1988.
[4] B.V. Babu, S. Gupta, Modeling and simulation for dynamic of packed bed adsorption, in: Proceedings of International Symposium & 57th Annual session of IIChE in Association with AIChE (CHEMCON-2004), Mumbai, December 27–30, 2004.
[5] H.T. Liao, C.Y. Shian, Analytical solution to an axial dispersion model for the fixed-bed adsorber, AIChE J. 46 (2000) 1168–1176.
[6] B.V. Babu, S. Gupta, Modeling and simulation of fixed bed adsorption column: effect of velocity variation, J. Eng. Technol. 1 (2005) 60–66.
[7] J.C. Crittenden, A.M. ASCE, W.J. Weber, Predictive model for design of fixed-bed adsorbers, J. Environ. Eng. Div. 104 (1978) 433–443.
[8] A.H. Sulaymon, K.W. Ahmed, Competitive adsorption of furfural and phenolic compound onto activated carbon in fixed bed column, Environ. Sci. Technol. 42 (2008) 392–397.
[9] J.A. Al-Najar, Removal of heavy metals by adsorption using activated carbon and kaolinite, Ph.D. Thesis, University of Technology, Baghdad, Iraq, 2009.
[10] E.J. Wilson, C.J. Geankoplis, Liquid mass transfer at very low Reynolds number in packed bed, Ind. Eng. Chem. Fundam. 5 (1966) 9–12.
[11] D.C. Ko, J.F. Porter, G. McKay, Film-pore diffusion model for the fixed-bed sorption of copper and cadmium Ions onto bone char, Water Res. 35 (2001) 3876–3886.
[12] T. Hang, Ion Exchange Modeling of Crystalline Silicotitanate Column for Cesium Removal From Argentine Waste, Wasting House Savannah River Company, 2003.
[13] K.K. Wong, C.K. Lee, K.S. Low, M.J. Haron, Removal of Cu and Pb from electroplating wastewater using tartaric acid modified rice hisk, Process Biochem. 39 (2003) 437–445.
[14] K.W. Ahmed, Removal of multi-pollutants from wastewater by adsorption method, Ph.D. Thesis, University of Baghdad, 2006.
[15] S.E. Ebrahim, Evaluation of a mixture adsorbent and glass bead for the removal of phenol and methylene blue from water, Ph.D. thesis, University of Baghdad, 2008.
[16] B.E. Reed, S. Arunachalam, B. Thomas, Removal of lead and cadmium from aqueous stream using granular activated carbon, Environ. Progr. 13 (1994) 60–64.
[17] E.H. Smith, A. Amini, Lead removal in fixed beds by recycled iron material, J. Environ. Eng. 12 (2000) 58–65.